Optics and Lasers in Engineering 110 (2018) 149–154

Contents lists available at ScienceDirect

Optics and Lasers in Engineering

journal homepage: www.elsevier.com/locate/optlaseng

A novel approach for measuring nanometric displacements by correlating speckle interferograms

Lucas P. Tendela*, Gustavo E. Galizzi

Instituto de Física Rosario, Blvd. 27 de Febrero 210 bis, Rosario S2000EZP, Argentina

ARTICLE INFO

Keywords:
Speckle interferometry
Phase evaluation
Nanometric displacements
Correlation coefficient

ABSTRACT

Recently, two phase evaluation methods were proposed to measure nanometric displacements by means of digital speckle pattern interferometry when the phase changes introduced by the deformation are in the range $[0, \pi)$ rad. However, one of these techniques requires separate recording of the intensities of the object and the reference beams which correspond to both the initial and the deformed interferograms. The other technique only works to measure out-of-plane displacements. In this paper, we present a novel approach that overcomes these limitations. The performance of the proposed method is analyzed using computer-simulated speckle interferograms and it is also compared with the results obtained with a phase-shifting technique. Finally, an application of the proposed phase method used to process experimental data is illustrated.

1. Introduction

Whole-field optical techniques can be used as useful tools to test micro-system devices due to their advantages, which include robustness, high processing speed, and also non-contact and non-destructive nature [1–6]. One of these optical techniques is digital speckle pattern interferometry (DSPI), which has a high sensitivity and also has been widely used for the measurement of displacement and strain fields generated by rough object surfaces [7]. This technique is based on the evaluation of the optical phase changes that are coded in speckle interferograms, which are usually displayed in the form of fringe patterns.

In practical applications of DSPI, the phase-shifting and the Fourier-transform methods are the most common techniques used to retrieve the phase distribution introduced by the deformation [8]. As it is well known, phase-shifting methods have high accuracy, and the sign ambiguity is resolved automatically due to the recording of multiple interferograms. However, a mirror driven by a linear computer-controlled piezoelectric transducer must be introduced in the optical setup, thus generating an additional technical complexity. Moreover, these algorithms assume that phase-shifts between successive frames are all equal, which can be difficult to obtain experimentally. Phase-shifter miscalibrations and vibrations during the acquisition of multiple speckle interferograms also produce systematic errors which must be appropriately addressed [9]. On the contrary, the Fourier transform method has the advantage of requiring the acquisition of only two speckle interferograms to be analyzed. Even so, when the phase changes are non-monotonous, this method also needs the introduction of spatial carrier fringes to overcome the sign ambiguity [8]. Although there exist simple ways of introducing spatial carrier fringes in the optical setup, such as tilting the reference beam between the acquisition of both speckle interferograms to be correlated, this procedure also complicates the automation of the interferometer operation.

A novel phase evaluation method was recently proposed to measure nanometric displacements by means of DSPI when the phase change introduced by the deformation is in the range $[0, \pi)$ rad, i.e., when the generated correlation fringes show less than one fringe [10]. In this case, the wrapped phase map does not present the usual 2π phase discontinuities, and it is therefore unnecessary to apply a spatial phase unwrapping algorithm to obtain the continuous phase distribution. It must be noted that cases of correlation fringe patterns presenting less than one fringe can appear quite frequently when micro-systems are inspected [11]. This phase retrieval method is based on the calculation of the local Pearson's correlation coefficient between the two speckle interferograms generated by both deformation states of the object. Although this approach does not need the introduction of a phase-shifting facility or spatial carrier fringes in the optical setup, the intensities of the object and the reference beams corresponding to both the initial and the deformed interferograms must be recorded. It should be noted that this limitation complicates the automation of the interferometer operation. Moreover, this limitation does not allow the application of this method for the analysis of non-repeatable dynamic events by recording a sequence of interferograms throughout the entire deformation history of the testing object.

More recently, Tendela et al. [12] have presented a phase retrieval method based on the approach reported in Ref. [10] to be used in a

* Corresponding author.
E-mail address: tendela@ifir-conicet.gov.ar (L.P. Tendela).

https://doi.org/10.1016/j.optlaseng.2018.05.023
Received 12 April 2018; Received in revised form 3 May 2018; Accepted 21 May 2018

DSPI. In this method there is no need to record the intensities of the object and the reference beams corresponding to both the initial and the deformed interferograms. However, when this technique is applied the rms phase errors for in-plane measurements are very large. Therefore, the approximations made in Ref. [12] are no longer valid for the in-plane case and this method is not suitable to measure in-plane displacements.

In this paper, we present a phase retrieval approach based on the methods reported in Ref. [10,12], which overcomes the aforementioned limitations. Therefore, there is no need to record the intensities of the object and the reference beams corresponding to both the initial and the deformed interferograms, and this technique can measure both in-plane and out-of-plane displacement fields. Furthermore, we show that the approximations made in Ref. [12] can be reached more naturally.

In the following section, a description of the proposed phase retrieval method is presented. Afterwards, the performance of the proposed method is analyzed using computer-simulated speckle interferograms for in-plane and of out-of-plane displacements. This analysis allows us to evaluate the rms phase errors introduced by the novel approach and also to compare its performance with the one given by a phase-shifting algorithm. Finally, an application of the phase retrieval method used to process experimental data is also illustrated.

2. Theorical concepts

As it is well known, DSPI is based on the recording of the coherent superposition of two optical fields, at least one of them being a speckle field generated by the scattered light coming from the rough surface of the specimen. The result of the superposition is another speckle field called interferogram and its intensity I can be expressed as [7]

$$I = I_1 + I_2 + 2\sqrt{I_1 I_2}\cos(\phi_1 - \phi_2) = I_0 + I_M \cos(\phi), \tag{1}$$

where I_1 and I_2 are the intensities of the object and the reference optical fields and ϕ_1 and ϕ_2 are their associated phases, respectively, $I_0 = I_1 + I_2$ is the intensity bias, $I_M = 2(I_1 I_2)^{1/2}$ is the modulation intensity, and $\phi = \phi_1 - \phi_2$ accounts for the optical path difference from the light source to the observation point considered.

If the scattering surface undergoes a deformation, the resulting intensity changes accordingly. The intensities I_a and I_b corresponding to the speckle interferograms recorded in the initial (a) and the deformed states (b), respectively, are determined by

$$\begin{aligned} I_a &= I_{a0} + I_{aM}\cos\phi_a = I_{a0} + I_{aM}\cos\phi_s \\ I_b &= I_{b0} + I_{bM}\cos\phi_b = I_{b0} + I_{bM}\cos(\phi_s + \Delta\phi), \end{aligned} \tag{2}$$

where $\phi_s = \phi_a$ accounts for the random change in the optical path due to the roughness of the scattering surface and $\Delta\phi = \phi_b - \phi_a$ corresponds to the deterministic change in the path introduced by the underwent deformation.

Below, it is presented a relationship to characterize the deterministic phase change $\Delta\phi$ as a function of the Pearson's correlation coefficient between the two interferograms described by Eq. (2). The Pearson's correlation coefficient $C(p, q)$ between two random variables p and q is defined as the covariance of the two variables divided by the product of their standard deviations and can be estimated as [13]

$$C(p,q) = \frac{\langle (p - \langle p\rangle)(q - \langle q\rangle)\rangle}{\left[(\langle p^2\rangle - \langle p\rangle^2)(\langle q^2\rangle - \langle q\rangle^2)\right]^{1/2}}, \tag{3}$$

where $\langle\ \rangle$ stands for the mean value of the sampled random variable.

Taking into account general hypotheses about the speckle distribution generated by the rough object, the correlation coefficient $C(I_a, I_b)$ for the two recorded interferograms I_a and I_b is given by

$$C = \frac{\langle (I_a - \langle I_a\rangle)(I_b - \langle I_b\rangle)\rangle}{[(\langle I_a^2\rangle - \langle I_a\rangle^2)(\langle I_b^2\rangle - \langle I_b\rangle^2)]^{1/2}}, \tag{4}$$

where the operator $\langle\ \rangle$ is evaluated by using a sliding window technique on each recorded image, and Eq. (2) can be used. The reader should note that the spatial coordinates of the pixel (m, n) at the CCD for $m, n = 1, \ldots, L$, where L is the number of pixels along the horizontal and vertical directions, were omitted intentionally for the sake of clarity.

Assuming that the intensity and phase of fully developed and polarized speckle fields are statistically independent, the following relationships are valid [14]

$$\begin{aligned} \langle I_M\cos\phi_s\rangle &= \langle I_M\rangle\langle\cos\phi_s\rangle, \\ \langle I_M\sin\phi_s\rangle &= \langle I_M\rangle\langle\sin\phi_s\rangle, \\ \langle I_M^2\sin^2\phi_s\rangle &= \langle I_M^2\cos^2\phi_s\rangle, \\ \langle\sin\phi_s\rangle &= \langle\cos\phi_s\rangle \approx 0, \\ \langle\sin\phi_s\cos\phi_s\rangle &\approx 0. \end{aligned} \tag{5}$$

In addition, considering that $\Delta\phi$ is a deterministic magnitude, and after some mathematical manipulations, the numerator N_{ab} of Eq. (4) can be expressed as a function of $\cos\Delta\phi$ as follows

$$N_{ab} = \langle I_{a0}I_{b0}\rangle - \langle I_{a0}\rangle\langle I_{b0}\rangle + \frac{1}{2}\langle I_{aM}I_{bM}\rangle\cos\Delta\phi. \tag{6}$$

In a similar way, the denominator D_{ab} of Eq. (4) can be computed as

$$D_{ab} = \left[\left(\langle I_{a0}^2\rangle - \langle I_{a0}\rangle^2 + \frac{1}{2}\langle I_{aM}^2\rangle\right)\times\left(\langle I_{b0}^2\rangle - \langle I_{b0}\rangle^2 + \frac{1}{2}\langle I_{bM}^2\rangle\right)\right]^{1/2}. \tag{7}$$

Replacing Eqs. (6) and (7) into Eq. (4), the correlation coefficient C can be estimated as

$$C(I_a, I_b) = \frac{\langle I_{a0}I_{b0}\rangle - \langle I_{a0}\rangle\langle I_{b0}\rangle + \frac{1}{2}\langle I_{aM}I_{bM}\rangle\cos\Delta\phi}{\left[(\langle I_{a0}^2\rangle - \langle I_{a0}\rangle^2 + \frac{1}{2}\langle I_{aM}^2\rangle)(\langle I_{b0}^2\rangle - \langle I_{b0}\rangle^2 + \frac{1}{2}\langle I_{bM}^2\rangle)\right]^{1/2}}. \tag{8}$$

Rearranging Eq. (8), the $\cos\Delta\phi$ can be written as

$$\begin{aligned} \cos\Delta\phi = C(I_a, I_b) &\times \frac{2\left[(\langle I_{a0}^2\rangle - \langle I_{a0}\rangle^2 + \frac{1}{2}\langle I_{aM}^2\rangle)(\langle I_{b0}^2\rangle - \langle I_{b0}\rangle^2 + \frac{1}{2}\langle I_{bM}^2\rangle)\right]^{1/2}}{\langle I_{aM}I_{bM}\rangle} \\ &- 2\frac{\langle I_{a0}I_{b0}\rangle - \langle I_{a0}\rangle\langle I_{b0}\rangle}{\langle I_{aM}I_{bM}\rangle}. \end{aligned} \tag{9}$$

As before, considering that the intensity bias and the modulation intensity of fully developed and polarized speckle fields are statistically independent, the following relationships are also valid [14]

$$\begin{aligned} \langle I_{a0}\rangle &= \langle I_{b0}\rangle = \langle I_0\rangle, \\ \langle I_{a0}I_{b0}\rangle &= \langle I_0^2\rangle, \\ \langle I_{a0}^2\rangle &= \langle I_{b0}^2\rangle = \langle I_0^2\rangle, \\ \langle I_{aM}\rangle &= \langle I_{bM}\rangle = \langle I_M\rangle, \\ \langle I_{aM}I_{bM}\rangle &= \langle I_M^2\rangle, \\ \langle I_{aM}^2\rangle &= \langle I_{bM}^2\rangle = \langle I_M^2\rangle. \end{aligned} \tag{10}$$

After some mathematical manipulations, the phase change $\Delta\phi$ needed to determine the displacement components can be evaluated by inverting Eq. (9) as follows

$$\Delta\phi = \operatorname{acos}\left[C(I_a, I_b)(\alpha + 1) - \alpha\right], \tag{11}$$

where acos[] is the inverse of the cosine function, and the coefficient α is defined as

$$\alpha = 2\frac{\langle I_0^2\rangle - \langle I_0\rangle^2}{\langle I_M^2\rangle}. \tag{12}$$

For further analysis, it will be useful to express the coefficient α as a function of the intensities of the object and reference fields I_1 and I_2

$$\alpha = \frac{\langle I_1^2\rangle - \langle I_1\rangle^2 + \langle I_2^2\rangle - \langle I_2\rangle^2}{2\langle I_1\rangle\langle I_2\rangle}. \tag{13}$$

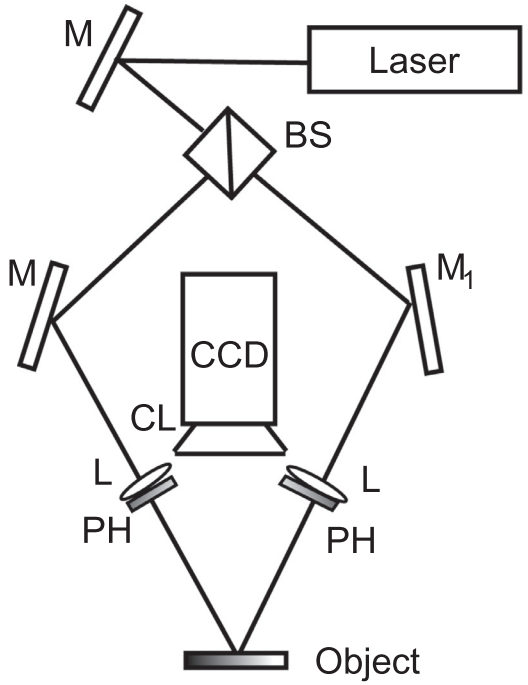

Fig. 1. Optical arrangement for measuring in-plane displacement using DSPII: mirrors (M), microscope objectives (L), beam splitters (BS), pin holes (PH), camera lens (CL).

2.1. Measurement of in-plane displacements

This subsection examines the statistical properties of the intensities of the object and reference fields for an optical configuration to measure in-plane displacements. In this case, Fig. 1 shows the two-beam arrangement described by Leendertz [15]. The surface under study is illuminated by two collimated beams of coherent light. These two beams generate their own speckle patterns I_1 and I_2, and there is no separate reference beam. Serving as references to each other, the pair of independent speckle patterns combines coherently to produce the resulting speckle pattern. If the intensities of I_1 and I_2 correspond to fully developed and polarized speckle fields, the following assumptions are made [14]

$$\langle I_1\rangle^2 = \langle I_1^2\rangle - \langle I_1\rangle^2,$$
$$\langle I_2\rangle^2 = \langle I_2^2\rangle - \langle I_2\rangle^2. \tag{14}$$

In addition, Jones et al. [16] has shown that this setup has better results when the ratio between the intensities I_1 and I_2 is equal to 1, i.e.$\langle I_1\rangle = \langle I_2\rangle$.

Therefore, for an in-plane configuration it can be shown that the coefficient defined in Eq. (13) results $\alpha_{IP} = 1$, and the phase change $\Delta\phi_{IP}$ can be measured as

$$\Delta\phi_{IP} = \operatorname{acos}\left[2C(I_a, I_b) - 1\right]. \tag{15}$$

2.2. Measurement of out-of-plane displacements

Fig. 2 shows a schematic view of an optical arragement for measuring out-of-plane displacements [16]. The outcoming beam from a laser source is divided into an object and reference beam. This reference beam is either a plane wave or another speckle field. The addition of a reference beam to the object wave introduces a significant change in the behavior of the resultant speckle pattern when the object is deformed. Since the resultant speckle pattern is formed by the interference of two coherent fields, the intensity in the pattern would naturally depend on whether a plane wave or a speckle field is used.

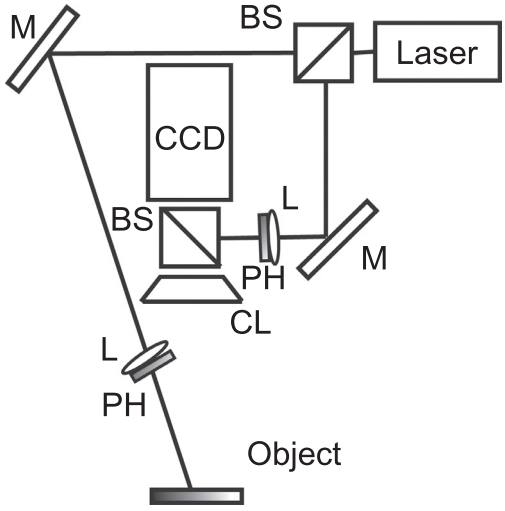

Fig. 2. Optical arrangement for measuring out-of-plane displacement using DSPI: mirrors (M), microscope objectives (L), beam splitters (BS), pin holes (PH), camera lens (CL).

2.2.1. One plane wave and one speckle field setup

In this case, the intensity I_1 is considered as the plane wave (reference beam), and the intensity I_2 is chosen as the speckle field (object beam). Therefore, the assumption $\langle I_2\rangle^2 = \langle I_2^2\rangle - \langle I_2\rangle^2$ is still valid [14]. Also, the ratio between the intensities I_1 and I_2 is equal to R, i.e.$\langle I_1\rangle = R\langle I_2\rangle$. Then, for an out-of-plane configuration where the reference beam is a plane wave, the following expression is valid $\langle I_1^2\rangle = \langle I_1\rangle^2$. Finally, it can be shown that Eq. (13) can be rewritten as $\alpha_{OP} = \frac{1}{2R}$, and the phase change $\Delta\phi_{OP}$ can be obtained as

$$\Delta\phi_{OP} = \operatorname{acos}\left[C(I_a, I_b)\left(\frac{1}{2R} + 1\right) - \frac{1}{2R}\right]. \tag{16}$$

2.2.2. Two speckle fields setup

Now, the reference beam I_1 is another speckle field, and I_2 is the intensity of the object beam, both of them corresponding to fully developed and polarized speckle fields. As before, the ratio between the intensities I_1 and I_2 is equal to R, i.e. $\langle I_1\rangle = R\langle I_2\rangle$, and the assumptions made in Eq. (14) are valid. Therefore, for an out-of-plane configuration where both beams are speckle fields, it can be shown that $\alpha_{OP} = \frac{1+R^2}{2R}$, and the phase change $\Delta\phi_{OP}$ can be evaluated as

$$\Delta\phi_{OP} = \operatorname{acos}\left[C(I_a, I_b)\frac{(1+R)^2}{2R} - \frac{1+R^2}{2R}\right]. \tag{17}$$

The validity of the proposed phase retrieval method will be demonstrated in Sections 3 and 4 by using numerical simulations and also experimental data.

3. Numerical results

The speckle interferograms used to evaluate the performance of the proposed phase retrieval technique were generated by computer-simulation. As described before, this approach allows to know precisely the original phase distribution and therefore, to determine the errors introduced by the algorithm used for evaluating the phase change. For this purpose, we used the same method to the one proposed in Ref. [10,12], which assumes that the speckle distribution generated by the rough object is fully developed.

As mentioned in Ref. [10,12], the proposed method does not generate phase values over the first and last L/2 pixels. As it was mentioned in these papers, it is not a trivial issue to ascertain the window size that must be used as it depends on the shape of the phase distribution to be evaluated. For the sake of clarity, in this paper we only show the results

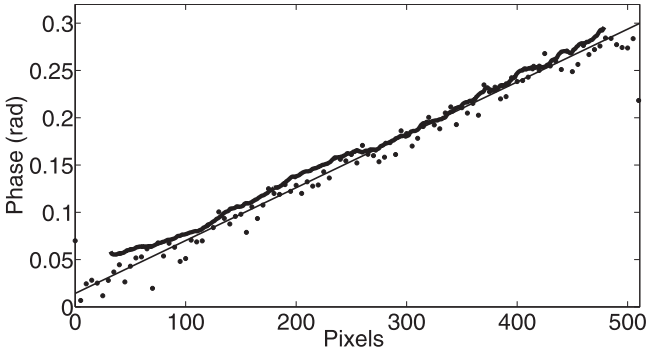

Fig. 3. Comparison between the original phase change (thin line) with the retrieved phase maps obtained using the proposed approach (bold line) and the Carré phase-shifting technique (solid circles) for a simulated in-plane tilt displacement.

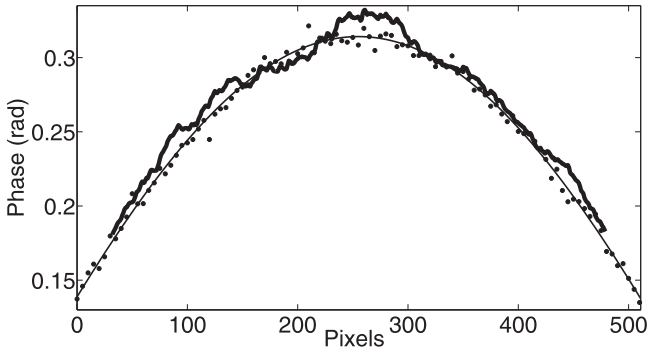

Fig. 4. Comparison between the original phase change (thin line) with the retrieved phase maps obtained using the proposed approach (bold line) and the Carré phase-shifting technique (solid circles) for a simulated out-of-plane parabolic displacement, using one plane wave and one speckle field setup.

Table 1
rms phase error σ using different simulated in-plane linear tilt distributions, and an average speckle size of 2 pixels.

$\Delta\phi$ (rad)	Original method σ (rad)	Novel method σ (rad)	Carré phase-shifting technique σ (rad)
$\pi/10$	0.0038	0.0059	0.0084
$\pi/4$	0.0110	0.0123	0.0175
$\pi/2$	0.0151	0.0234	0.0323

obtained using a sliding window of size $L^2 = 65 \times 65$ pixels. The effects of different window sizes were deeply analyzed in Ref. [10,12].

3.1. Numerical results for measuring in-plane displacements

The proposed phase retrieval method was tested using different simulated phase distributions. As a typical example, Fig. 3 shows the retrieved phase distribution obtained with the proposed approach (bold curve) along a direction crossing the center of the pattern for an in-plane tilt displacement. In this example, the highest phase change between the initial and deformed states was chosen as $\Delta\phi = \pi/10$ rad, and the average speckle size was set in 2 pixels. For comparison, the same figure also displays the original input phase map (thin curve) and the phase distribution (solid circles) retrieved by means of the Carré phase-shifting technique.

As previously mentioned, the rms phase error σ was used to evaluate the performance of the proposed phase retrieval method. In this case, the novel approach outperforms the Carré phase-shifting technique, as it gives $\sigma = 0.0059$ rad compared to a value of 0.0084 rad that was obtained using the conventional approach. For comparison, the rms phase error was also computed using the original method (the one reported in Ref. [10]), giving $\sigma = 0.0038$ rad.

Furthermore, the coefficient α defined in Eq. (13) was also computed for each pixel (m, n) in the example displayed in Fig. 3, using the intensities of the object and the reference beams which correspond to both the initial and the deformed interferograms. The obtained results showed that the rms deviation evaluated between α and the approximated value of 1 was 0.009. Therefore, the substitution of $\alpha_{IP} = 1$ in Eq. (11) can be considered as very accurate.

The performance of the novel phase retrieval approach was also analysed using different phase amplitudes and average speckle sizes. Some of the results obtained from this numerical analysis are summarized in Tables (1) and (2). Several interesting observations emerge from the numerical tests. Looking the numerical results listed in Table (1), it should be noted that the rms phase errors generated by the proposed approach are larger than the ones obtained using the original method. However, the novel approach still outperforms the Carré phase-shifting technique. Table (2) shows the rms phase errors σ using different average speckle sizes. The highest phase change between the initial and deformed states was chosen as $\pi/10$ rad. For an average speckle size of 1 pixel, the proposed approach did not recover the phase change properly. This is due to the fact that the intensities I_1 and I_2 do not correspond to fully developed and polarized speckle fields.

3.2. Numerical results for measuring out-of-plane displacements

3.2.1. One plane wave and one speckle field setup

Fig. 4 depicts the retrieved phase distribution (in bold line) of an out-of-plane parabolic displacement obtained using the proposed approach, and evaluated along a line crossing the center of the pattern. In this second example, the average speckle size was set in 2 pixels. The highest phase change between the initial and deformed states was chosen as $\Delta\phi = \pi/10$ rad, and the ratio intensities between I_1 and I_2 was $R = 2$. For comparison, the same figure also shows the original input phase map (thin line) and the phase distribution obtained using the Carré phase-shifting technique (solid circles). Here, the performances of both approaches were quite similar, as the rms phase error obtained with the proposed phase retrieval method was $\sigma = 0.0062$ rad and with the Carré phase-shifting technique was $\sigma = 0.0045$ rad.

The coefficient α defined in Eq. (13) was also computed for each pixel (m, n) in the example displayed in Fig. 4, using the intensities of the object and the reference beams which correspond to both the initial and the deformed interferograms. The obtained results showed that the rms deviation evaluated between α and the approximated value of $1/2R$ was 0.009. Therefore, the substitution of $\alpha_{OP} = \frac{1}{2R}$ in Eq. (11) can be considered as accurate.

By using different ratio intensities between I_1 and I_2, the performance of the phase retrieval approach was also analysed. Looking the numerical results listed in Table (3), it should be noted that the rms phase errors generated by the proposed approach are quite similar to the one obtained with the Carré phase-shifting technique.

3.2.2. Two speckle fields setup

In this example, the correlation was also evaluated using an average speckle size of 2 pixels, and the highest phase change between the initial and deformed states was chosen as $\Delta\phi = \pi/10$ rad. The ratio intensities between I_1 and I_2 was $R = 2$. Fig. 5 shows the phase distribution obtained with the proposed method (in bold line) of an out-of-plane parabolic displacement and evaluated along a line crossing the center of the pattern. For comparison, the same figure also shows the original input phase map (thin line) and the phase distribution obtained using the Carré phase-shifting technique (solid circles). As before, the performances of both approaches were quite similar, as the rms phase error obtained with the proposed phase retrieval method was $\sigma = 0.0053$ rad and with the Carré phase-shifting technique was $\sigma = 0.0064$ rad.

Table 2
rms phase error σ for simulated in-plane linear tilt distributions of $\pi/10$, and using different average speckle sizes.

Average speckle size (pixels)	Original method σ (rad)	Novel method σ (rad)	Carré phase-shifting technique σ (rad)
1	0.0018	0.0149	0.0038
2	0.0038	0.0059	0.0084
3	0.0048	0.0067	0.0134
4	0.0086	0.0099	0.0152
5	0.0085	0.0092	0.0182

Table 3
rms phase error σ using different ratio intensities R corresponding to out-of-plane parabolic distributions (maximun phase values of $\pi/10$) for one plane wave and one speckle field, with an average speckle size of 2 pixels.

R	Original method σ (rad)	Novel method σ (rad)	Carré phase-shifting technique σ (rad)
2	0.0051	0.0062	0.0045
4	0.0046	0.0059	0.0044
8	0.0053	0.0040	0.0044

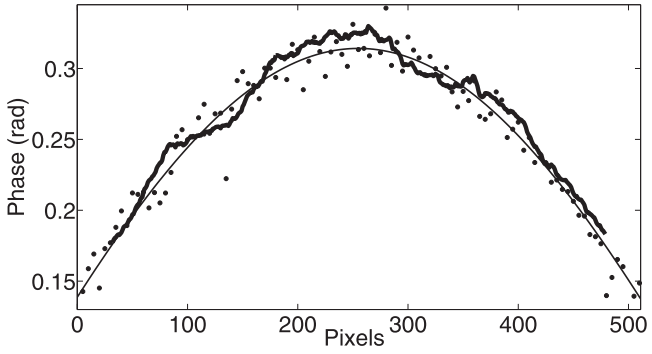

Fig. 5. Comparison between the original phase change (thin line) with the retrieved phase maps obtained using the proposed approach (bold line) and the Carré phase-shifting technique (solid circles) for a simulated out-of-plane parabolic displacement, using two speckle fields setup.

Table 4
rms phase error σ using different ratio intensities R corresponding to out-of-plane parabolic distributions (maximun phase values of $\pi/10$) for two speckle fields, with an average speckle size of 2 pixels.

R	Original method σ (rad)	Novel method σ (rad)	Carré phase-shifting technique σ (rad)
2	0.0051	0.0053	0.0064
4	0.0046	0.0062	0.0080
8	0.0043	0.0068	0.0090

In this case, the coefficient α was also computed for each pixel (m, n). The obtained results show that the rms deviation evaluated between α and the approximated value of 1.25 was 0.01. Therefore, the substitution of $\alpha_{OP} = \frac{1+R^2}{2R}$ in Eq. (11) can be considered as accurate.

The performance of the novel phase retrieval approach was also analysed using different ratio intensities between I_1 and I_2. Some of the results obtained from this numerical analysis are summarized in Table (4). As before, the rms phase errors generated by the proposed approach are quite similar to the one obtained with the Carré phase-shifting technique.

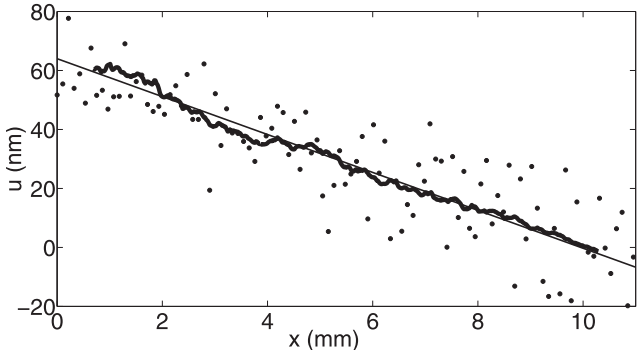

Fig. 6. In-plane displacement field u along a line crossing the center of the steel plate obtained using the proposed approach (bold line), with its linear fit (thin line) and the Carré phase-shifting technique (solid circles).

4. Experimental results

To illustrate the performance of the novel phase retrieval method when experimental data are processed, a DSPI system was used to measure the in-plane horizontal displacement component u produced by a steel plate when it was rotated around a fixed horizontal axis using a differential micrometer. Fig. 1 shows a schematic view of the DSPI system, which was based on a conventional in-plane speckle interferometer illuminated by a Nd:YAG laser with a wavelength $\lambda = 532.8$ nm, which was divided into two beams by a 50/50 beam-splitter (BS). Both beams are expanded by two microscope objectives (L) and illuminate the specimen making an angle $\gamma = 45°$ with respect to the normal of the surface. In order to obtain a uniform illumination intensity, a pin hole (PH) was used in both beams. The specimen is imaged by a PULNIX TM-620 CCD camera, whose output was fed to a frame grabber located inside a personal computer that digitizes the images in grey levels with a resolution of 512×512 pixels $\times$ 8 bits. The video camera had a zoom lens which allows to image a small region of the specimen of approximately 11×11 mm^2 in size and for an average speckle size of 3 pixels.

A piezoelectric transducer attached to the mirror (M_1) and driven by an electronic unit was used to introduce the phase shifts. This phase-shifting facility enabled to evaluate the phase distribution using the Carré phase-shifting technique, which later was compared with the phase map obtained using the novel method. With both phase retrieval methods, the proposed approach and the Carré phase-shifting technique, the in-plane horizontal displacement component u was determined using [17]

$$u = \frac{\lambda}{4\pi \sin\gamma} \Delta\phi. \tag{18}$$

Fig. 6 depicts the displacement component u measured with the novel method (bold curve) along a line crossing the center of the aluminium plate. This figure shows that the maximum in-plane displacement generated by the plate is 63 nm. As previously mentioned, the proposed method does not give phase values over the first and the last 32 pixels due to the size of the sliding window used to calculate the correlation. The same figure also shows the linear fit (in thin line) ob-

tained from a least square calculation of the measured data. Despite some scatter, it is observed that this line fits quite well with the measurements. For comparison, the same figure also displays the in-plane displacement component obtained with the Carré phase-shifting technique (solid circles). The results shown in this last figure demonstrate that the performances given by both processing approaches are quite similar, and confirm the simplicity and accuracy of the proposed phase retrieval method to measure displacement fields in the nanometer range.

In addition, to evaluate the accuracy of the approximation $\alpha_{IP} = 1$ when experimental data was processed, the intensities of the object and the reference beams corresponding to both the initial and the deformed interferograms were separately recorded. In this case, the obtained results showed that the rms deviation evaluated between α_{IP} and the assumed value of 1 was 5×10^{-3}, demonstrating the validity of the approximation introduced in Section 2.

Finally, the displacement uncertainty does not only depend on the error introduced by the novel method used to estimate the phase distribution but also on the relative contribution of various error sources, such as the direction of the sensitivity vector and its variation across the specimen, the CCD noise and the intensity fluctuations of the laser [8,18].

5. Conclusions

In this paper we propose a novel method to be used in DSPI for measuring nanometric displacement fields when the phase change varies in the range [0, π) rad. The proposed phase evaluation method is based on the local calculation of the correlation between the two speckle interferograms generated by both deformation states of the object. This approach does not need the introduction of a phase-shifting facility or spatial carrier fringes in the optical setup to measure the phase distributions generated by the object deformation without any sign ambiguity. Additionally, this technique can measure both in-plane and out-of-plane displacement fields.

The performance of the proposed method is investigated using different computer-simulated phase distributions, approach which allows to evaluate the rms phase errors. The numerical analysis shows that the performance of the proposed method is quite similar to the one given by the Carré phase-shifting technique. Although the rms errors obtained by the approach reported in Ref [10]. are slightly lower than those generated by the proposed method, when this last simplified approach is applied it is not necessary to record separately the intensities of the object and the reference beams corresponding to both the initial and the deformed interferograms. This advantage not only makes easier the automation of the interferometer operation, but also allows the application of the novel method to the analysis of non-repeatable dynamic events by recording a sequence of interferograms throughout the entire deformation history of the testing object. Finally, the results given by the numerical analysis are confirmed by processing experimental data obtained from the tilt displacement of an aluminium plate. The experimental results demonstrate that the performances of the proposed phase retrieval method and the Carré phase-shifting technique are quite similar, and also confirm the simplicity of the proposed method to measure displacement fields in the nanometer range.

References

[1] Osten W. Optical inspection of microsystems. Boca Raton: Taylor & Francis; 2007.
[2] Vogel D, Kühnert R, Michel B. Strain measurement in micrometrology. proc int conf on advanced photonic sensors and applications. In: Proc SPIE, 3897. Singapore; 1999. p. 224–38.
[3] Kumar UP, Bhaduri B, Mohan NK, Kothiyal MP, Asundi AK. Microscopic TV holography for MEMS deflection and 3-d surface profile characterization. Opt Lasers Eng 2008;46:687–94.
[4] Mohan NK, Rastogi PK. Recent developments in interferometry for microsystems metrology. Opt Lasers Eng 2009;47:199–202.
[5] Kumar UP, Mohan NK, Kothiyal MP. Measurement of static and vibrating microsystems using microscopic TV holography. Optik 2011;122:49–54.
[6] Asundi A. Digital holography for MEMS and microsystem metrology. Chichester: Wiley; 2011.
[7] Rastogi PK. Digital speckle pattern interferometry and related techniques. Chichester: Wiley; 2001.
[8] Huntley JM. Automatic analysis of speckle interferograms. In: Rastogi P K, editor. Digital speckle pattern interferometry and related techniques. Chichester, New York: Wiley; 2001, p. 59139.
[9] Huntley JM. Automated fringe pattern analysis in experimental mechanics: a review. J Strain Anal 1998;33:105–25.
[10] Tendela LP, Galizzi GE, Federico A, Kaufmann GH. Measurement of nanometric displacements by correlating two speckle interferograms. Appl Opt 2011;50:1758–64.
[11] Höfling R, Aswendt P. Speckle metrology for microsystem inspection. In: Osten W, editor. Optical inspection of microsystems. Boca Raton: Taylor & Francis; 2007. p. 427–58.
[12] Tendela LP, Galizzi GE, Federico A, Kaufmann GH. A fast method for measuring nanometric displacements by correlating speckle interferograms. Opt Lasers Eng 2012;50:170–5.
[13] Jobson JD. Applied multivariate data analysis volume I: regression and experimental design. New York: Springer-Verlag; 1991.
[14] Goodman JW. Statistical properties of laser speckle patterns. In: Dainty JC, editor. Laser speckle and related phenomena. Berlin: Springer-Verlag; 1975. p. 9–75.
[15] Leendertz JA. Interferometric displacement measurement on scattering surfaces utilizing speckle effect. J Phys E 1970;3:214–18.
[16] Jones R, Wykes K. Holographic and speckle interferometry. Cambridge: Cambridge University Press; 1989.
[17] Rastogi PK. Measurement of static surface displacements, derivatives of displacements and three dimensional surface shape. In: Rastogi PK, editor. Digital speckle pattern interferometry and related techniques. Chichester, New York: Wiley; 2001. p. 142–224.
[18] Kaufmann GH, Albertazzi A. Speckle interferometry for the measurement of residual stresses. In: Caulfield HJ, Vikram CS, editors. New directions in holography and speckle. California: American Scientific Publishers; 2008. p. 353–74.